DFT Calculations and Spectral Measurements of Charge-Transfer Complexes Formed by Aromatic Amines and Nitrogen Heterocycles with Tetracyanoethylene and Chloranil

Meng-Sheng Liao, Yun Lu, Vernon D. Parker, and Steve Scheiner*

Department of Chemistry & Biochemistry, Utah State University, Logan, Utah 84322-0300

Received: April 11, 2003; In Final Form: July 21, 2003

Charge-transfer (CT) spectra of the $\pi-\pi$ complexes formed by several aromatic amines and nitrogen heterocycles [acting as donors (Ds)] with acceptor A [A = tetracyanoethylene (TCNE), chloranil (CA)] were measured in acetonitrile. Density functional theory (DFT) calculations were then carried out in solvent to determine the probable geometric structures of the complexes that are responsible for the absorption bands. Three aspects of the intermolecular association were investigated: the D−A separations and relative orientations of the D and A, the D−A binding energies, and the excitation energies of transitions from the HOMO of D to the LUMO of A. On the basis of the calculated results, which are in good agreement with experiment, the nature and origins of the CT spectra of the various molecular complexes are clarified.

1. Introduction

Intermolecular charge-transfer (CT) complexes are formed when electron donors (D) and electron acceptors (A) interact, a general phenomenon in organic chemistry.[1] Mulliken[2] considered such complexes to arise from a Lewis acid−Lewis base type of interaction, the bond between the components of the complex being postulated to arise from the partial transfer of a π electron from the base (D) to orbitals of the acid (A). In solution, the composition of the complexed species could be represented by a 1:1 molar ratio,[3] and the association equilibrium may be written as

$$D + A \overset{K_{DA}}{\rightleftharpoons} D-A$$

One characteristic feature of a D−A complex is the appearance of a new absorption band in the spectrum of the complex, commonly attributed to an intermolecular CT transition, involving electron transfer from the donor to the acceptor. (The term "CT complex" is misleading in that very little charge is actually transferred in the ground state for such complexes.[4])

The nature of intermolecular CT complexes has been the subject of many investigations. Early work in this field was based mainly on Mulliken's valence bond theory[2] in which the D−A complex is described as a resonance hybrid of an uncharged aggregate (D, A) and an ionic structure (D^+-A^-) formed by charge transfer from D to A. This theory was able to provide an adequate explanation of many spectroscopic results and to predict the most stable complex geometries. However, it is not sufficient to consider only CT interactions when describing the properties of the complexes in which this interaction is not the dominant contribution to the ground-state stabilization. More detailed theoretical studies[5−7] indicated that contributions from different types of interactions (electrostatic, charge-transfer, exchange repulsion, and polarization) are all important. Experimental results also suggested that the D−A partners at close separation are held together mainly by van der Waals-type forces.[8]

Accurate descriptions of the bonding properties of weakly bound systems have proven to be a challenge to theoretical researchers.[9] The Hartree−Fock (HF) method is clearly inadequate because of its failure to account for electron correlation and dispersion. Ab initio studies require the use of high-quality correlated methods (e.g., CCSD-T, CASPT2, etc.);[10,11] such calculations remain very time-consuming and impractical for large molecular systems.

Density functional theory (DFT) is an attractive alternative to conventional ab initio methods because it provides an estimate of the correlation energy at a relatively modest cost. However, the DFT methods depend on an adequate exchange-correlation (XC) potential. By a series of educated trials and errors, more and more accurate XC forms have been developed,[12−19] and now DFT enjoys widespread use in the calculations of various types of bonding (including van der Waals molecules and hydrogen bonds). There have been several papers[18−20] assessing DFT for some simple $C_2H_4-X_2$ or NH_3-X_2 (X = halogen) CT complexes, showing that hybrid DFT methods, in which the (exact) HF exchange is mixed in the exchange density functional, can provide remarkably accurate results for the properties considered.

Because of their wide application and use (ranging from chemistry, materials science, and medicine to biology), CT complexes have attracted considerable research interest, and over the years, a very large number of CT complexes have been prepared and experimentally studied.[21] One problem of great interest is their conformation in the ground state. Many molecular complexes cannot be fully isolated and so must be studied in solution. There has been considerable discussion about the relative orientation of the D and A components in certain D−A complexes in solution, with conflicting data reported, and considerable uncertainty remains as to the exact geometry of the complexes.[22] Moreover, the spectra of some CT complexes contain two bands (or more) that may be associated with transitions from the two highest occupied orbitals of D to the lowest unoccupied orbital of A or with the existence of two distinct complex geometries (orientational isomers). The origins of such multiple absorption bands have also been the subject of investigations.[23−26]

Tetracyanoethylene (TCNE) and chloranil (CA) (Figure 1, part II) are strong electron acceptors that form complexes with a variety of donors. This work concerns the formation of CT

* Corresponding author. E-mail: scheiner@cc.usu.edu.

10.1021/jp034985t CCC: $25.00
Published on Web 10/01/2003

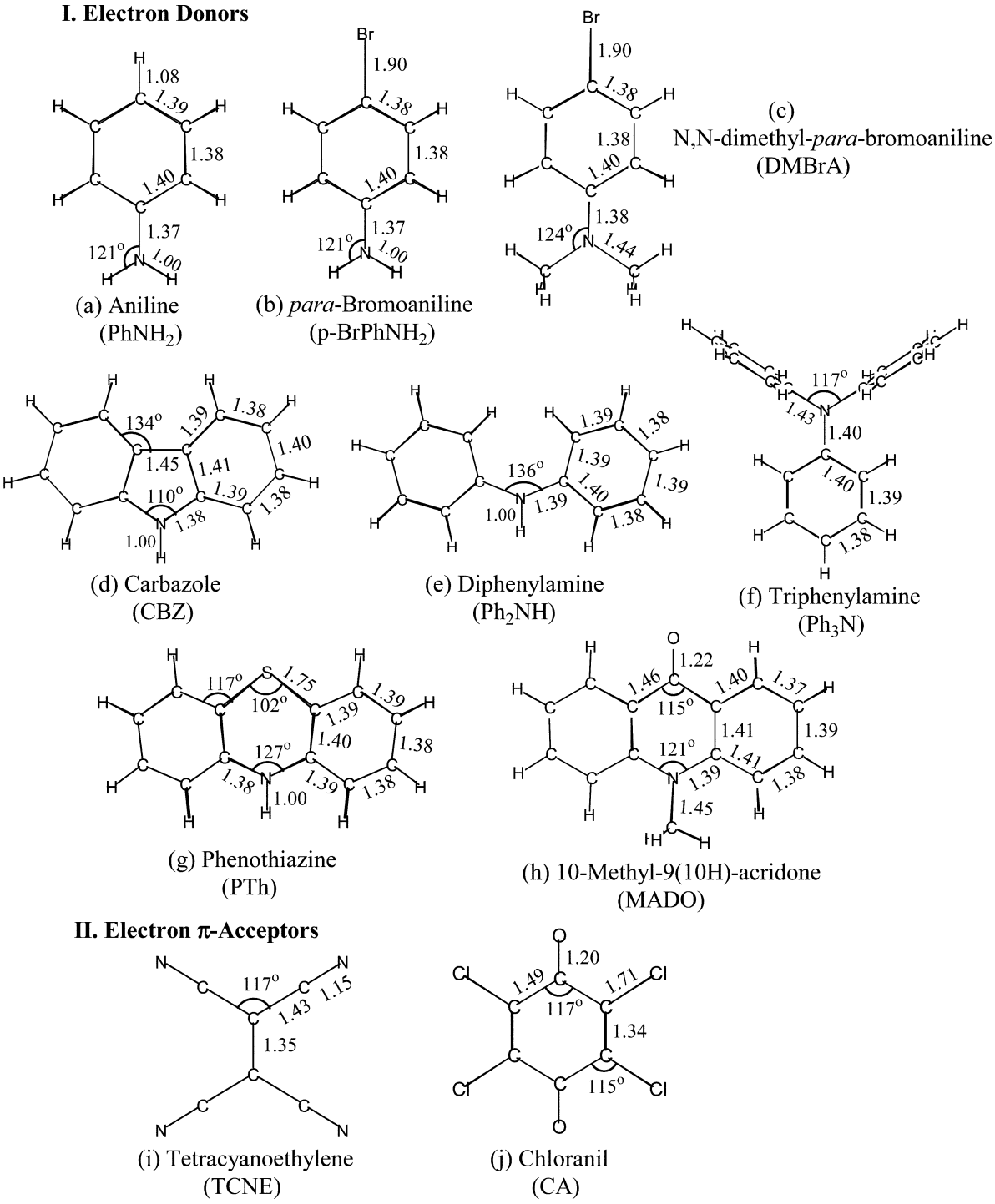

Figure 1. Molecular structures of the electron donors (D, part I) and acceptors (A, part II), along with the optimized values of selected bond lengths (in Å) and bond angles. (The solvent field has a small, nearly negligible effect on the molecular structure of the individual molecules.).

complexes of several aromatic amines and nitrogen heterocycles with TCNE and with CA. DFT calculations have been carried out in solvent in order to understand the energetics and origin of the CT spectra. By calculating electron excitation energies (E^{exc}) and D−A binding energies (E_{bind}), the most probable geometric structures of the complexes that are responsible for the absorption bands are determined.

2. Experimental and Computational Details

The electron donors chosen for study are illustrated in Figure 1. On the basis of the molecular structure and type, these donor molecules may be classified into four groups. Group 1 [aniline ($PhNH_2$), *para*-bromoaniline (*p*-$BrPhNH_2$), and *N,N*-dimethyl-*para*-bromoaniline (DMBrA)] contain only one benzene ring; *p*-$BrPhNH_2$ and DMBrA are derivatives of $PhNH_2$. The N atom connects two benzene rings in group 2 [carbazole (CBZ) and diphenylamine (Ph_2NH)]. CBZ differs from Ph_2NH in that the rings in the former are joined together by a second covalent bond as well. Both molecules are planar, owing to conjugation effects. Triphenylamine belongs to group 3, where the N atom connects three phenyls. To avoid strong steric interactions, two phenyl rings are twisted so that they are nearly perpendicular to the plane of the other phenyl ring. Phenothiazine (PTh) and 10-methyl-9(10H)-acridone (MADO) are anthracene-like molecules that belong to group 4.

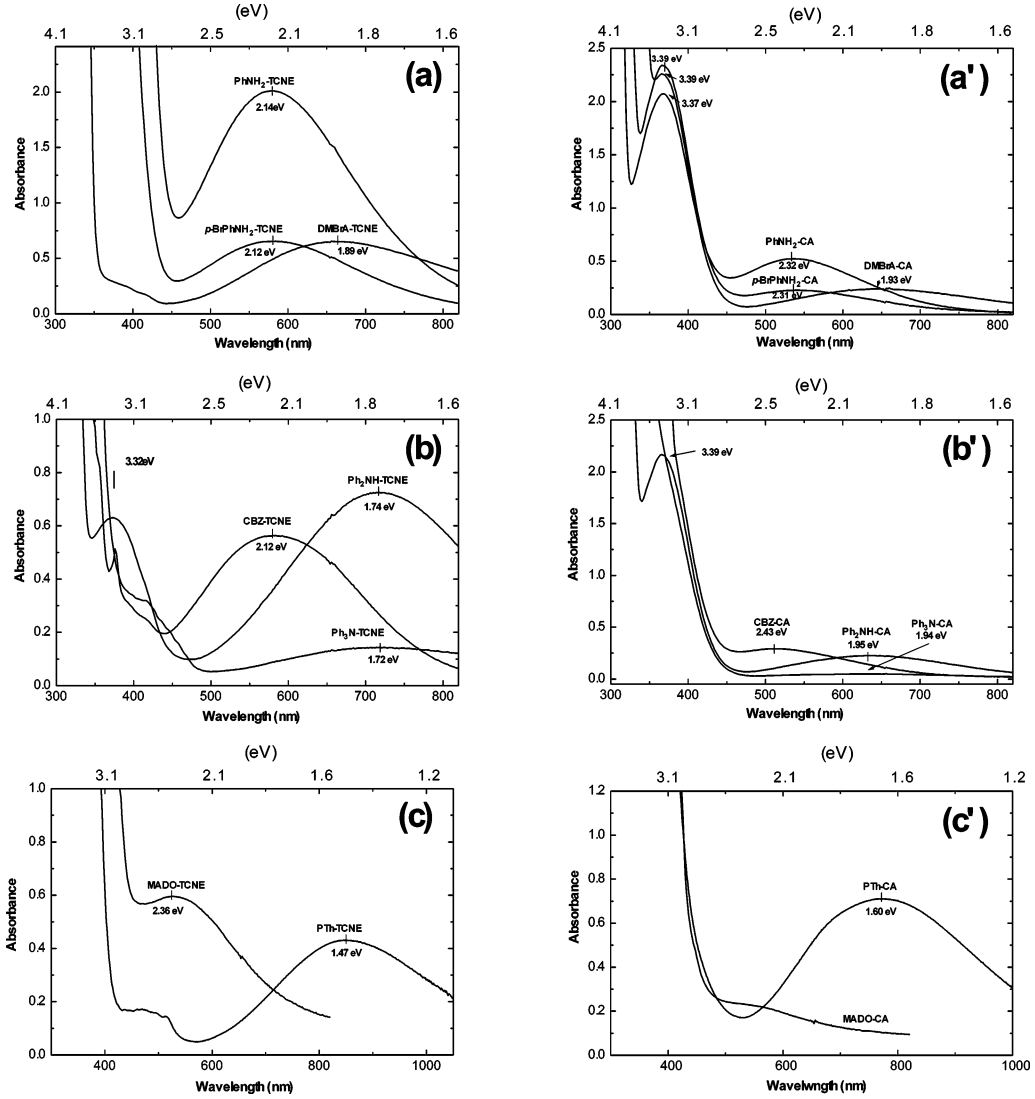

Figure 2. Measured charge-transfer (CT) spectra of the D−TCNE (left) and D−CA (right) complexes in acetonitrile. The concentrations of the substances are TCNE, 0.0125 M; CA, 0.025 M; $PhNH_2$, 0.0625 M; *p*-$BrPhNH_2$, 0.0312 M; DMBrA, 0.0312 M; CBZ, 0.0312 M; Ph_2NH, 0.0625 M; Ph_3N, 0.0625 M; PTh, 0.0312 M; and MADO, 0.100 M.

All chemicals were purchased from Aldrich and Acros and purified by standard procedures before use. Except for PTh-A (A = TCNE, CA), the UV−vis absorption spectra for the D−A complexes in acetonitrile were obtained with a Hewlett-Packard 8452 diode array spectrometer. The spectra of PTh−TCNE and PTh−CA were obtained with a Hewlett-Packard 8453 spectrometer. All spectra (Figure 2) were recorded soon after the two substrate solutions were mixed.

All calculations were carried out using the Gaussian 98 program package.[27] To simulate the effects of the polar solvent, self-consistent reaction field (SCRF) calculations were carried out using a polarized continuum (overlapping spheres) model (PCM).[28] The density functional that was used was based on the combination of Becke's half (-HF) and half (-DFT) exchange[15] with the correlation functional of Lee, Yang, and Parr (LYP).[13] A systematic test of various density functionals (including several recently developed ones) was performed previously on some $\pi-\pi$ CT complexes,[29] and it was shown that this hybrid BH&HLYP functional provides satisfactory excitation energies and also in other ways furnishes the best performance for describing the properties of $\pi-\pi$ CT complexes in general. Because the solvent field is shown to have only very small effects on the calculated excitation energies (vide infra), the conclusion drawn in ref 29 also holds for the DFT calculations in solution. The basis set employed was the standard 6-31G*, which has been shown to be adequate for calculations on weakly bound CT complexes.[29] Larger basis sets have also been tested for two of the CT systems so as to gauge the influence of basis-set size. As may be seen in Table 1, there is

TABLE 1: Calculated Properties[a] of $PhNH_2$−TCNE and $PhNH_2$−CA with Different Basis Sets

D−A complex	basis set	R_{D-A} (Å)	Δ_{LU-HO} (eV)	E^{exc} (eV)	*f*	E_{bind} (kcal/mol)
$PhNH_2$−TCNE	6-31G*	3.33	3.55	1.88	0.0577	7.00
	6-31+G*	3.40	3.49	1.82	0.0440	5.64
	6-311G*	3.33	3.53	1.85	0.0515	6.84
	6-311+G*	3.36	3.51	1.83	0.0461	6.26
$PhNH_2$−CA	6-31G*	3.53	3.85	2.21	0.0465	4.37
	6-31+G*	3.64	3.83	2.19	0.0328	3.57
	6-311G*	3.46	3.92	2.25	0.0507	4.89
	6-311+G*	3.52	3.90	2.24	0.0408	4.71

[a] R_{D-A}, intermolecular distance between D and A (see Figures 3 and 4); E^{exc}, excitation energy; *f*, oscillator strength; E_{bind}, binding energy between D and A [$-E_{bind} = E(D-A) - E(D) - E(A)$]. Solvent effects are not included.

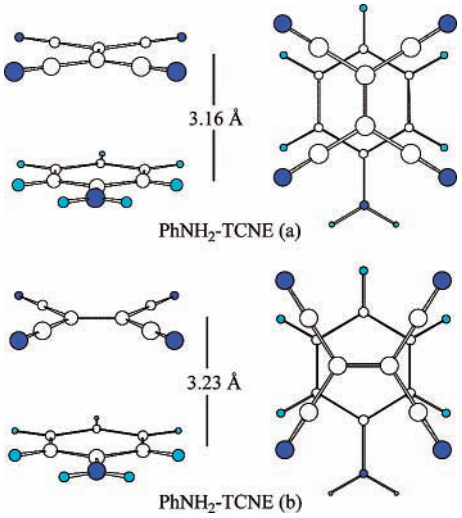

Figure 3. Two distinct conformations of $PhNH_2-TCNE$.

fairly close agreement between the 6-31G* and 6-311+G* calculations.

Electron excitation energies related to the absorption spectra were calculated using the time-dependent density functional response theory (TDDFT) as recently implemented in the Gaussian program. TDDFT provides a first-principles method for the calculation of excitation energies and represents an excellent alternative to conventional highly correlated CI methods. Applications of TDDFT to excitation energy calculations can be found in recent work.[29−32]

3. Results and Discussion

Selected bond lengths and angles, optimized for the isolated donor and acceptor molecules, are reported in Figure 1. (The solvent field has a small, nearly negligible effect upon the molecular structures of the isolated molecules.) Upon pairing to form a CT complex, the principle of maximum overlap would lead one to expect a conformation wherein the planes of the donor and acceptor molecules lie parallel to one another in a stacked arrangement. Indeed, this structure has been observed in the solid state.[1,33−35] A similar structural arrangement is believed to occur in solution as well. The geometric parameter of particular interest in the stacked structure is the intermolecular distance R_{D-A} (separating the parallel D and A planes). There are a number of geometric possibilities for the D−A complexes. (The internal geometries of the subunits remain nearly unaffected in the complex.[29,36,37]) Consideration has been limited to those alignments of D and A that provide the greatest overlap and that are usually discussed in the literature. These structures are illustrated in Figures 3−6 for the D−TCNE complexes; conformations considered for D−CA are analogous.

The calculated properties of the D−A complexes, with A = TCNE and CA, are collected in Tables 2 and 3, respectively. Excitation energies (E^{exc}) refer to the lowest transitions, along with their oscillator strengths, f. The D−A binding energy, E_{bind}, is defined as the difference between the total energy of the complex (in solvent) and the sum of the individual components (in solvent). These properties are tabulated without counterpoise corrections for basis set superposition error (BSSE), followed by the calculated BSSEs in the last column of each Table.

Figure 7 illustrates how the molecular orbitals (MOs) of each donor D combine with those of TCNE when the complex is formed. (The MO energy-level diagrams of D−CA are similar to those of D−TCNE.) Because of the weakness of the D−A interaction, only minor perturbations are observed in the energies of the subunit orbitals, which involve a (slight) upward shift of the acceptor orbitals coupled with a downshift of the donor orbitals. Because the HOMO (as well as HOMO-1, etc.) and LUMO of the complex are associated with D and A components, respectively, an electron transition from the HOMO to the LUMO leads to a new absorption band.

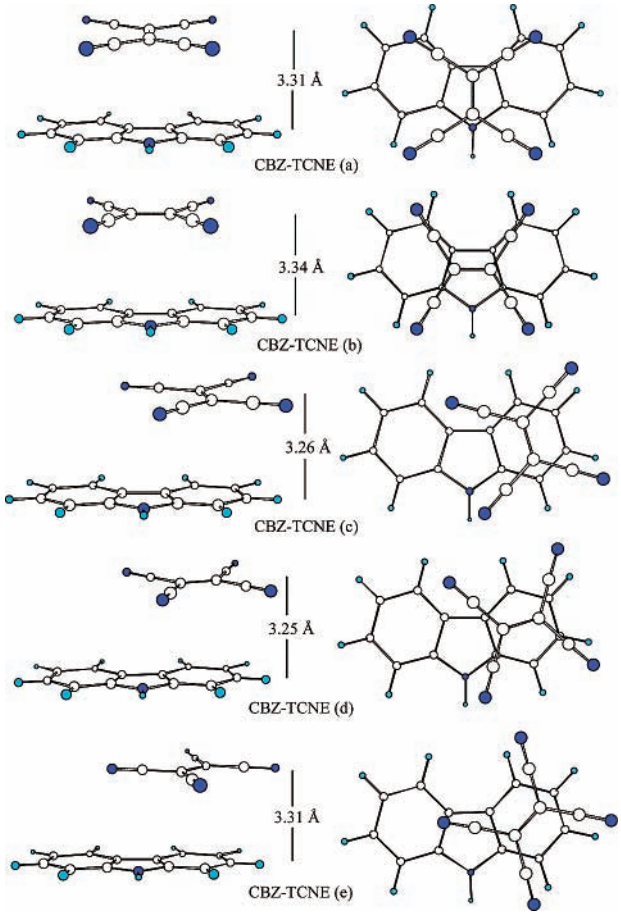

Figure 4. Five distinct conformations of CBZ−TCNE.

3.1. Basis Set Effects. An accurate calculation of a molecular system requires the use of basis sets of sufficient size and flexibility, but an overly large set can create computational problems. It therefore becomes important to identify an optimal basis set, one of manageable size but also one that provides reliable calculated properties. The effects of adding diffuse functions to the basis set (6-31+G*) and using the larger triple-ζ basis sets (6-311G*, 6-311+G*) were carefully assessed, using $PhNH_2-TCNE$ and $PhNH_2-CA$ as prototypes (without considering solvent effects).

A comparison of results obtained with these different basis sets is reported in Table 1. The calculated intermolecular distance (R_{D-A}) varies somewhat with the basis set. Adding diffuse functions to 6-31G* lengthens the D−A distance by 0.07 and 0.11 Å in $PhNH_2-TCNE$ and $PhNH_2-CA$, respectively. The enlargement of the valence segment has a different effect; R_{D-A} remains unchanged for $PhNH_2-TCNE$ on going from 6-31G* to 6-311G* but is shortened by 0.07 Å for $PhNH_2-CA$. After the valence space has been enlarged to 6-311G*, the addition of diffuse functions continues to elongate R_{D-A}, but by a smaller amount. For both systems, the 6-31G* values of R_{D-A} are close to those obtained by 6-311+G*, undoubtedly because of a certain amount of error cancellation in 6-31G*.

The calculated LUMO−HOMO energy gap and the associated excitation energy are less sensitive to the choice of basis

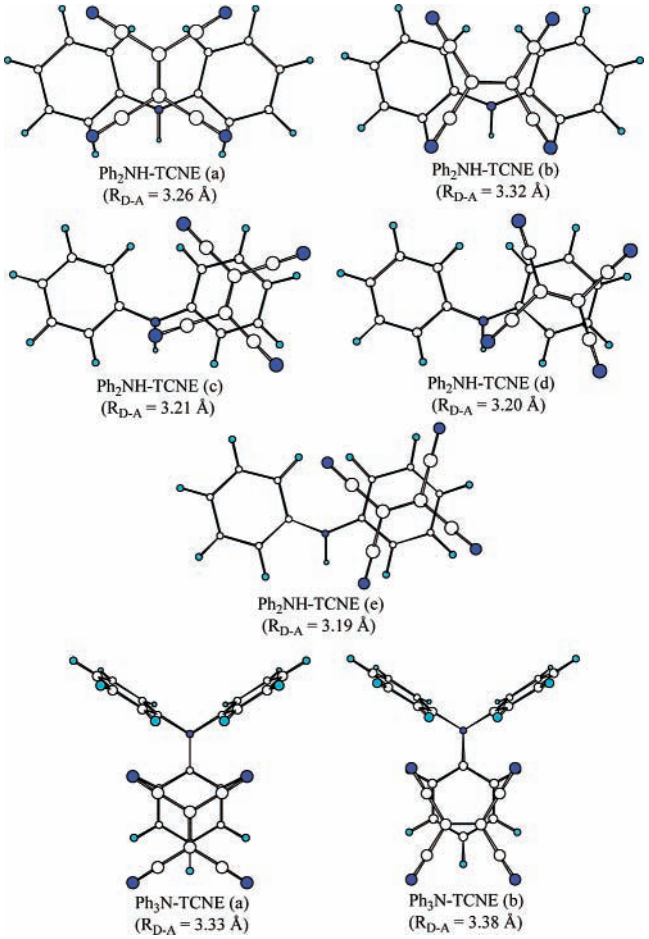

Figure 5. Five distinct conformations of $Ph_2NH-TCNE$ and two conformations of $Ph_3N-TCNE$.

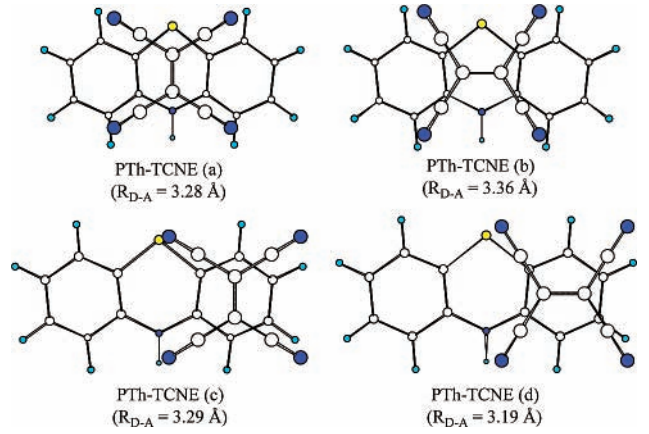

Figure 6. Four distinct conformations of PTh−TCNE.

set; the variations of E^{exc} are less than 0.1 eV. The calculated oscillator strengths, *f*, are lowered by the inclusion of diffuse functions, but enlarging the valence space does not have a consistent effect. The same is true for the binding energies, where the addition of diffuse functions leads to a decrease in this quantity, but this reduction is of a smaller magnitude for the triple-ζ set. Again, the transition from 6-31G* to 6-311G* does not have a consistent effect.

In summary, the 6-31G* basis set appears to be sufficiently reliable to provide reasonable results for the CT complexes, and the larger basis sets do not significantly affect the molecular properties in a qualitative way.

3.2. Solvent Effects. To assess the effects of solvent on the calculated properties, calculations were also performed on *free* D−A complexes (i.e., D−A in the gas phase). The differences in the results (Δ) between solvated and free D−A complexes are presented in Table 4. Upon solvation, the binding energy of the various complexes decreases by 1−2 kcal/mol in the majority of cases, and the equilibrium D−A distance is diminished by 0.2−0.3 Å. Most importantly for our purposes, the excitation energy is scarcely affected by solvation; the deviation from the gas-phase E^{exc} is 0.1 eV or less.

In summary, the D−A complex is stabilized by the polar solvent, which gives rise to a shortening of the D−A distance. However, the binding energy of D−A in the solvent is decreased, owing to the greater stabilizations of the isolated components. Concerning the excitation energy, the solvent effect on E^{exc} is quite small.

3.3. D-TCNE (D = $PhNH_2$, *p*-$BrPhNH_2$, DMBrA). Two distinct conformations were considered for these complexes, as shown in Figure 3. In conformation **a**, the TCNE double bond is parallel to the line connecting the 1,4-carbon atoms in the benzene ring, whereas the two are perpendicular in conformation **b**. Geometry optimizations indicate that the center of TCNE lies over the center of the benzene ring in either case. The calculated D−A distances for the two complexes are very close. R_{D-A} is equal to 3.16 Å in **a** and is slightly longer, 3.23 Å, in **b**. It is hence not surprising that **a** is more stable by some 1.0 kcal/mol. The introduction of the electron-withdrawing Br, which pulls electron density out of the ring, reduces the stability of the complex by ~1 kcal/mol. In contrast, the addition of electron-donating CH_3 groups to the N atom (DMBrA) increases the binding energy of the D−A complex. In all three of these complexes, it is structure **a** that is the more stable.

The HOMO → LUMO transition in $PhNH_2-TCNE$ **a** is calculated to be 1.90 eV with $f = 0.082$. The HOMO-1 → LUMO transition (3.02 eV) is symmetry-forbidden for this conformation. The same is true for the other two complexes. For the less-stable **b** conformations, however, the situation is reversed, and it is the HOMO-1 → LUMO transition that is allowed and the HOMO → LUMO transition that is forbidden. Our experimental spectrum of $PhNH_2-TCNE$ shows a broad, intense band with a peak at 2.14 eV that we attribute to the HOMO → LUMO transition in **a**. The very strong absorption background at higher energy (>3.1 eV) prohibits the elucidation of any details there. Frey et al.[24] reported an earlier spectral measurement of $PhNH_2-TCNE$ in dichloromethane, which contained two strong bands at 2.10 and 3.22 eV. The former band is consistent with our interpretation of a HOMO → LUMO transition in **a**, and the latter is most likely associated with the allowed HOMO-1 → LUMO transition of **b**, which is calculated to occur at 3.03 eV. This simultaneous observation of both conformers is consistent with the small energy difference separating them.

The lowest excitation energy obtained for *p*-$BrPhNH_2-TCNE$ is nearly the same as that of $PhNH_2-TCNE$, both theoretically and experimentally. However, this quantity is substantially diminished for D = DMBrA. This pattern is consistent with the destabilization of the donor 3a′ HOMO by the electron-donating CH_3 substituents, as evident in Figure 7. Whereas the Br on the ring has little effect on the HOMO energy, the lower-lying orbitals (e.g., HOMO-1) are shifted a good deal. The excitation energies of the HOMO-1→LUMO transition are hence rather different for $PhNH_2$ and *p*-$BrPhNH_2$, but because these transitions are forbidden for the energetically preferred **a** conformations, these differences are not apparent in the experimental spectrum. Compared with the experimental spectra,

TABLE 2: Calculated Properties of CT Complexes Involving TCNE in Acetonitrile[a] Solvent

D−A complex[b]	R_{D-A} (Å)	transition[c] (singlet → singlet)	E^{exc} (eV) calcd	E^{exc} (eV) exptl[d]	f	E_{bind} (kcal/mol)	BSSE[e] (kcal/mol)
$PhNH_2$−TCNE(a)	3.16	HO → LU	1.90	2.14	0.0820	5.00	−2.30
		HO-1 → LU	3.02		0.0001		
***p*-BrPhNH_2−TCNE(a)**	3.15	HO → LU	1.89	2.12	0.0691	4.29	−2.81
		HO-1 → LU	3.30		0.0001		
DMBrA−TCNE(a)	3.17	HO → LU	1.60	1.89	0.0528	4.53	−3.12
		HO-1 → LU	3.25		0.0001		
CBZ−TCNE(a)	3.31	HO → LU	1.81		0.0529	1.89	−2.30
		HO-1 → LU	1.90		0.0006		
		HO-2 → LU	3.11		0.0088		
CBZ−TCNE(b)	3.34	HO → LU	1.61		0.0020	1.69	−2.16
		HO-1 → LU	1.96		0.0328		
		HO-2 → LU	3.11		0.0111		
CBZ−TCNE(c)	3.26	HO → LU; HO-1 → LU	1.86		0.0161	3.37	−2.31
		HO → LU; HO-1 → LU	2.09		0.0375		
		HO-2 → LU	3.37		0.0380		
Ph_2NH−TCNE(a)	3.26	HO → LU	1.33		0.0549	2.55	−2.34
		HO-1 → LU	2.73		0.0040		
Ph_2NH−TCNE(b)	3.32	HO → LU	1.18		0.0031	1.31	−2.09
		HO-1 → LU	2.97		0.0028		
Ph_2NH−TCNE(c)	3.21	HO → LU	1.52		0.0374	3.66	−2.21
		HO-1 → LU; HO-2 → LU; HO-3 → LU	3.18		0.0350		
Ph_3N−TCNE(a)	3.33	HO → LU	1.58	1.72	0.0340	1.95	−2.41
		HO-1 → LU; HO-2 → LU; HO-3 → LU	2.78		0.0000		
		HO-1 → LU; HO-3 → LU	3.08		0.0001		
PTh−TCNE(a)	3.28	HO → LU	0.85		0.0010	1.33	−2.19
		HO-1 → LU	2.46		0.0547		
		HO-2 → LU	3.34		0.0096		
PTh−TCNE(b)	3.36	HO → LU	0.75		0.0012	0.82	−1.93
		HO-1 → LU	2.24		0.0002		
		HO-2 → LU	3.28		0.0009		
MADO−TCNE(a)	3.67	HO → LU	1.66		0.0208	0.73	−2.28
		HO-1 → LU	3.06		0.0004		
MADO−TCNE(b)	3.69	HO → LU	1.60		0.0006	0.80	−2.09
		HO-1 → LU	3.08		0.0096		
$PhNH_2$−TCNE(b)	3.23	HO → LU	1.49		0.0002	3.98	−2.19
		HO-1 → LU	3.03		0.0679		
p-Br$PhNH_2$−TCNE(b)	3.25	HO → LU	1.54		0.0001	3.17	−2.66
		HO-1 → LU	3.30		0.0576		
DMBrA−TCNE(b)	3.27	HO → LU	1.28		0.0000	3.63	−2.77
		HO-1 → LU	3.26		0.0550		
CBZ−TCNE(d)	3.25	HO → LU	1.85	2.12	0.0127	3.81	−2.29
		HO-1 → LU	2.16		0.0801		
		HO-2 → LU	3.30		0.0038		
CBZ−TCNE(e)	3.31	HO → LU	1.80		0.0108	3.01	−2.18
		HO-1 → LU	2.08		0.0501		
		HO-2 → LU	3.30		0.0184		
Ph_2NH−TCNE(d)	3.20	HO → LU	1.62	1.74	0.0622	4.01	−2.22
		HO-1 → LU; HO-3 → LU	3.18	3.32	0.0218		
Ph_2NH−TCNE(e)	3.19	HO → LU	1.57		0.0500	3.62	−2.29
		HO-1 → LU; HO-2 → LU; HO-3 → LU	3.09		0.0008		
Ph_3N−TCNE(b)	3.38	HO → LU	1.44		0.0000	1.44	−2.36
		HO-1 → LU; HO-2 → LU; HO-3 → LU	2.81		0.0322		
		HO-3 → LU; HO-1 → LU; HO-3 → LU	3.05		0.0024		
PTh−TCNE(c)	3.29	HO → LU	0.95		0.0022	1.32	−1.94
		HO-1 → LU; HO-3 → LU	2.58		0.0655		
		HO-2 → LU	3.55		0.0022		
PTh−TCNE(d)	3.19	HO → LU	1.44	1.47	0.1509	2.78	−2.11
		HO-1 → LU; HO-3 → LU	2.68		0.0035		
		HO-2 → LU	3.79		0.0079		
MADO−TCNE(c)	3.30	HO → LU	1.83	2.36	0.0169	1.84	−2.20
		HO-1 → LU; HO-2 → LU;	3.23		0.0223		
		HO-4 → LU					
MADO−TCNE(d)	3.31	HO → LU	1.82		0.0244	1.43	−2.18
		HO-1 → LU; HO-2 → LU; HO-4 → LU	3.20		0.0316		

[a] Dielectric constant $\epsilon = 36.64$. [b] For the various D−A structures considered, see Figures 3−6; the most probable structure is indicated in bold. [c] HO = HOMO (HO-1 is the second HOMO, etc.), and LU = LUMO; (HO → LU; HO-1 → LU) represents configuration mixing between HO → LU and HO-1 → LU transitions. [d] The experimental data refer to the absorption maxima in the absorption spectra. [e] The calculated BSSEs are not included in the E_{bind}'s.

the calculated E^{exc} values appear to be uniformly underestimated by about 0.3 eV.

3.4. CBZ−TCNE. The CT complexes of carbazole derivatives with organic acceptors have attracted considerable interest as useful organic photoconductors. There have been several investigations[24,38−40] on the CBZ−TCNE complex with the aim of understanding the energies and types of CT transitions. Calculations were carried out on five possible conformations, illustrated in Figure 4. Both **a** and **b** center the TCNE above the central ring of CBZ, and both belong to the C_s point group. In conformations **a** and **b**, the C═C bond of TCNE is perpendicular and parallel, respectively, to the CBZ long axis.

TABLE 3: Calculated Properties[a] of CT Complexes Involving CA in Acetonitrile[b] Solvent

D−A complex	R_{D-A} (Å)	transition (singlet → singlet)	E^{exc} (eV) calcd	E^{exc} (eV) exptl	f	E_{bind} (kcal/mol)	BSSE (kcal/mol)
$PhNH_2$−CA (a)	3.29	HO → LU	2.20	2.32	0.0827	2.12	−2.29
		HO-1 → LU; HO-2 → LU	3.19		0.0001		
$PhNH_2$−CA (b)	3.34	HO → LU	1.91	3.37	0.0001	2.00	−2.19
		HO-1 → LU	3.44		0.0491		
***p*-$BrPhNH_2$−CA (a)**	3.18	HO → LU	2.40	2.31	0.1130	0.30	−3.44
		HO-1 → LU; HO-2 → LU	3.40		0.0000		
p-$BrPhNH_2$−CA (b)	3.29	HO → LU	1.93	3.39	0.0000	0.24	−3.15
		HO-1 → LU; HO-2 → LU	3.59		0.0477		
DMBrA−CA (a)	3.31	HO → LU	2.04	1.93	0.0653	1.89	−3.76
		HO-1 → LU; HO-3 → LU	3.39		0.0000		
DMBrA−CA (b)	3.51	HO → LU	1.78	3.39	0.0000	1.84	−2.93
		HO-1 → LU	3.70		0.0305		
CBZ−CA (a)	3.63	HO → LU	2.07		0.0059	0.07	−1.99
		HO-1 → LU	2.28		0.0003		
		HO-2 → LU; HO-3 → LU	3.46		0.0002		
CBZ−CA (b)	3.58	HO → LU	2.13		0.0005	0.99	−2.59
		HO-1 → LU	2.44		0.0408		
		HO-2 → LU; HO-3 → LU	3.57		0.0003		
CBZ−CA (c)	3.71	HO → LU; HO-1 → LU	2.19		0.0046	1.81	−2.02
		HO → LU; HO-1 → LU	2.42		0.0055		
		HO-2 → LU; HO-3 → LU	3.56		0.0002		
CBZ−CA (d)	3.62	HO → LU	2.17		0.0054	2.05	−2.21
		HO-1 → LU	2.44		0.0315		
		HO-2 → LU; HO-3 → LU	3.49		0.0009		
CBZ−CA (e)	3.61	HO → LU	2.30	2.43	0.0201	2.16	−2.10
		HO-1 → LU	2.44		0.0115		
		HO-2 → LU; HO-3 → LU	3.53		0.0014		
Ph_2NH−CA (a)	3.70	HO → LU	1.72		0.0105	0.37	−1.92
		HO-1 → LU; HO-3 → LU; HO-4 → LU	3.35		0.0006		
Ph_2NH−CA (b)	3.73	HO → LU	1.71		0.0011	0.52	−2.39
		HO-1 → LU; HO-6 → LU; HO-7 → LU; HO-9 → LU	3.52		0.0030		
Ph_2NH−CA (c)	3.34	HO → LU	1.86		0.0089	1.36	−2.06
		HO-1 → LU; HO-2 → LU; HO-3 → LU; HO-4 → LU	3.34		0.0063		
Ph_2NH−CA (d)	3.33	HO → LU	1.88	1.95	0.0219	1.35	−2.07
		HO-1 → LU; HO-3 → LU; HO-4 → LU	3.32	3.39	0.0065		
Ph_2NH−CA (e)	3.36	HO → LU	1.91		0.0441	1.32	−2.18
		HO-1 → LU; HO-2 → LU; HO-3 → LU; HO-4 → LU	3.32		0.0004		
Ph_3N−CA (a)	3.37	HO → LU	1.96	1.94	0.0436	2.36	−3.21
		HO-1 → LU; HO-2 → LU; HO-3 → LU; HO-6 → LU	3.07		0.0002		
Ph_3N−CA (b)	4.34	HO → LU	2.02		0.0000	0.01	−0.68
		HO-1 → LU; HO-2 → LU; HO-3 → LU	3.33		0.0040		
PTh−CA (a)	3.74	HO → LU	1.27		0.0001	0.01	−1.79
		HO-1 → LU	2.78		0.0051		
		HO-2 → LU; HO-3 → LU; HO-4 → LU	3.44		0.0000		
PTh−CA (b)	3.81	HO → LU	1.30		0.0003	0.04	−2.06
		HO-1 → LU	2.79		0.0000		
		HO-2 → LU; HO-3 → LU; HO-4 → LU	3.56		0.0000		
PTh−CA (c)	3.81	HO → LU	1.39		0.0002	1.03	−1.62
		HO-1 → LU; HO-3 → LU	2.90		0.0107		
		HO-2 → LU; HO-3 → LU; HO-4 → LU	3.52		0.0000		
PTh−CA (d)	3.66	HO → LU	1.46	1.60	0.0212	1.27	−1.91
		HO −1 → LU; HO-2 → LU; HO-3 → LU	2.86		0.0003		
		HO-2 → LU; HO-3 → LU; HO-4 → LU	3.58		0.0001		

[a] See legends of Tables 1 and 2. [b] Dielectric constant $\epsilon = 36.64$.

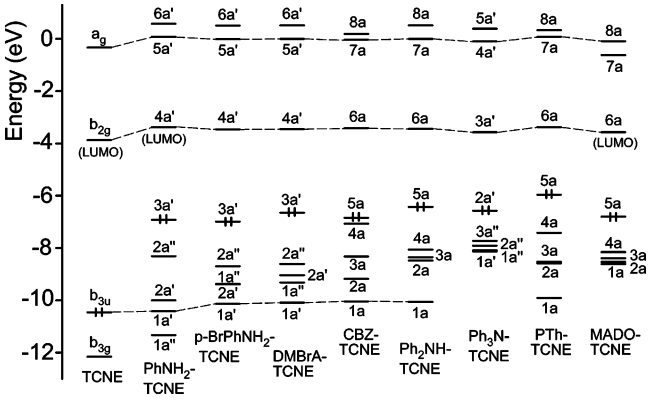

Figure 7. MO energy-level diagrams of CT complexes involving TCNE. The orbitals of the acceptor (TCNE) are connected by dashed lines.

Conformations **c**, **d**, and **e** place TCNE above one of the CBZ phenyl rings, in various orientations. The calculated binding energies indicate that this latter location, above a phenyl ring, provides better $\pi-\pi$ electron interaction and is thus energetically favorable to **a** and **b**. It might be observed that the calculated values of R_{D-A} are directly related to the D−A binding strength. That is, the most strongly bound complexes are associated with shorter intermolecular separations.

According to our measurements (Figure 2b), the absorption maximum of the CT spectrum occurs at 2.12 eV. Previous detailed inspections and analyses[24,25,38−40] reveal that the single broad band is composed of two strongly overlapping bands (CT1, CT2), which arise from transitions between the HOMO and HOMO-1 of CBZ and the LUMO of TCNE. (Experimental data[38] have ruled out the possibility that CT1 and CT2 arise from different isomers.) The calculations on symmetric (C_s) structures **a** and **b** indicate only one low-energy CT band that involves the HOMO (or HOMO-1) of CBZ, consistent with previous analyses[25,38] based on the symmetries of D and A orbitals. This contrast with the spectral observation, when coupled with the higher energies of these two conformers, would effectively appear to rule out their presence. Indeed, Raman spectroscopic studies[38] support this notion, arguing that the most probable geometry for the complex of CBZ−TCNE is asymmetric.

Owing to the low degree of symmetry in **c**−**e**, both CT transitions HOMO → LUMO and HOMO-1 → LUMO are optically allowed. The computed excitation energies and oscillator strengths are quite similar from one of these conformations to the next and so offer little means of identifying the one that is present. The calculated energetics indicate that the preferred conformation is **d**, wherein the TCNE C═C bond bifurcates C−C bonds within the phenyl, leading to the conclusion that **d** is most likely to be observed. It should be noted that its calculated excitation energy of 1.85 eV is close to the observed value of 2.12 eV.

According to the calculation, the energy splitting between the CT1 and CT2 excitations is ∼0.3 eV, and the lower-energy transition (CT1) has a smaller oscillator strength (*f*) than does CT2. By fitting to their resonance Raman data, Egolf et al.,[38] assigned the stronger transition to CT1. Okamoto[39] and Klöpffer,[40] however, arrived at the opposite conclusion concerning these relative strengths; they obtained their best fits with CT2 assigned as the stronger band. The calculations support the assignment of the latter authors. Finally, a weak absorption peak appears near 3.35 eV; calculations suggest that this peak is associated with the HOMO-2 → LUMO transition of conformer **d** (3.30 eV, $f = 0.0038$).

3.5. $Ph_2NH-TCNE$. The conformations considered for $Ph_2NH-TCNE$ (Figure 5) are similar to those of CBZ−TCNE. Geometries **a** and **b** do not effectively overlap the D and A orbitals, as indicated by their relatively small binding energies and long R_{D-A}. As in the case of carbazole, conformation **d** is found to be the most stable. In contrast to CBZ−TCNE, the spectrum of $Ph_2NH-TCNE$ contains two widely separated, broad, intense bands whose maxima are located at 1.74 and 3.32 eV, respectively. Only the HOMO → LUMO transition of **a** carries a large *f* value (0.0549), whereas **b** is associated with two weak transitions ($f \approx 0.003$), so these two structures can effectively be ruled out. The calculated data of **d** conform remarkably well to the experimental spectrum. The HOMO → LUMO band occurs at 1.62 eV, and the HOMO-1 → LUMO band occurs at 3.18 eV, in good agreement with the observed peaks at 1.74 and 3.32 eV, respectively. Moreover, the oscillator strengths suggest reasonably strong absorption bands. Rotating the two molecules relative to one another leads to structure **e**, with only a small loss in stability. However, this rotation effectively causes the second band to vanish ($f = 0.0008$), so this conformation is inconsistent with the experimental spectrum.

3.6. $Ph_3N-TCNE$. It is reasonable to assume that the acceptor lies over one of the rings of the triphenylamine donor. Two distinct conformations for $Ph_3N-TCNE$ were considered, as shown in the lower part of Figure 5. Because of the strong steric interaction from the other two perpendicular phenyls, TCNE is shifted (by ∼0.9 Å) away from the benzene center. Structure **a** is computed to be energetically preferable to **b**, and it also has a shorter R_{D-A}. The spectrum exhibits a maximum near 1.72 eV with relatively small absorption strength. The excitation energy of the HOMO → LUMO transition in **a** is computed to be 1.58 eV with $f = 0.034$, in nice agreement with the experimental spectrum. The same HOMO → LUMO transition is forbidden in **b**, for which the allowed transition would correspond to HOMO-1 → LUMO with $E^{exc} = 2.81$ eV, much higher than the observed frequency. These results would suggest that despite the energetic and geometric similarities of conformations **a** and **b** only the former is present in solution.

3.7. PTh−TCNE and MADO−TCNE. Phenothiazine has attracted considerable attention as a drug molecule and can participate in CT complex formation with simple acceptor molecules. Spectral measurements of PTh−TCNE and PTh−CA were described in the early literature.[41] MADO is structurally similar, as evident in Figure 1. Four distinct conformations were considered for both PTh−TCNE and MADO−TCNE, illustrated in Figure 6. The TCNE lies above the central ring in **a** and **b** but over a peripheral ring in **c** and **d**.

A strong absorption maximum occurs for PTh−TCNE near 1.47 eV, together with a broad shoulder having a maximum near 2.82 eV. Of the four conformations considered, it is only the spectral data for **d** that is consistent with this experimental information. The low-energy, strong absorption may be attributed to the HOMO → LUMO transition ($E^{exc} = 1.44$ eV, $f = 0.1509$), and the HOMO-1 → LUMO transition ($E^{exc} = 2.68$ eV, $f = 0.0035$) can be connected with the shoulder. Reassuringly, this same conformation **d** was found to be clearly preferred on energetic grounds as well.

The situation is somewhat different for MADO−TCNE, where **c** is (slightly) more stable than **d** energetically. However, the calculated spectral values of **c** and **d** are similar and in reasonable accord with the experimental spectrum. It may not be possible to assign the observed spectrum unambiguously to either **c** or **d**, which allows the possibility of free rotation of the TCNE.

TABLE 4: Solvent Effects on Calculated Properties[a] [$\Delta X = X$(in solvent) − X(in gas phase)]

		D = $PhNH_2$	*p*-$BrPhNH_2$	DMBrA	CBZ	Ph_2NH	Ph_3N	PTh	MADO
A = TCNE	ΔE_{bind}	−2.00	−1.88	−1.14	−1.94	−1.63	−3.15	−2.44	−2.21
	ΔR_{D-A}	−0.17	−0.18	−0.17	−0.18	−0.20	−0.32	−0.27	−0.21
	ΔE^{exc}	0.02	0.02	0.03	−0.02	0.07	0.12	0.10	0.09
A = CA	ΔE_{bind}	−2.25	−3.67	−2.47	−1.17	−1.67	−3.21	−1.22	
	ΔR_{D-A}	−0.24	−0.31	−0.16	−0.07	−0.28	−0.27	−0.03	
	ΔE^{exc}	−0.01	0.07	0.03	−0.04	−0.03	0.05	−0.03	

[a] D−A binding energy E_{bind} in kcal/mol, D−A distance R_{D-A} in Å, and excitation energy E^{exc} in eV. Values refer to the lowest-energy geometry of each complex.

3.8. Complexes with CA. The spectra of the complexes involving chloranil are significantly different than for TCNE, as a comparison of the left and right sides of Figure 2 will attest. The complexes selected for computation for the D−CA complexes are analogous to those investigated for D−TCNE and are illustrated in Figures 3−6.

Two CT bands are clearly observed in the spectra of $PhNH_2$−, *p*-$BrPhNH_2$−, and DMBrA−CA. Because the calculations indicate that there is only one allowed excitation for either structure **a** or **b**, the two bands are attributed to a mixture of two isomeric conformers. Indeed, the calculated lowest excitation energies of the three complexes are all in very good agreement with the experimental spectra, the errors being less than 0.15 eV. The HOMO-1 → LUMO excitations are also in good agreement with the second observed band, albeit with a generally larger discrepancy.

As in the TCNE case, conformations **c**, **d**, and **e** of CBZ−CA are energetically preferred to **a** and **b**. However, unlike CBZ−TCNE where **d** was clearly the most stable, there is no such differentiation possible in CBZ−CA, suggesting that all three isomers could coexist in solution with almost equal probability. However, structure **c** does not produce a strong CT absorption because all three calculated *f* values are very small. Both **d** and **e** give rise to two allowed CT transitions, arising from HOMO → LUMO and HOMO-1 → LUMO. The spectrum of CBZ−CA appears as a single broad band with a maximum near 2.43 eV, and thus it is likely a composite of two overlapping bands, similar to the case of CBZ−TCNE. According to the calculation, the HOMO → LUMO transition is weaker than the HOMO-1 → LUMO transition for **d**, but the opposite is true for **e**. In summary, it is possible that all three conformations **c**, **d**, and **e** might coexist in solution, and it is further clear that **c** will not be present exclusive of the others.

As in the case of Ph_2NH−TCNE, the **c**, **d**, and **e** structures are energetically preferred over **a** and **b** for Ph_2NH−CA. The experimental spectrum of the latter contains two CT bands at 1.95 and 3.39 eV. The calculated excitation energies of the former three conformations are all similar, but the oscillator strengths of **d** match the spectrum most closely. The values of *f* are very small for both transitions in **c**, and the second oscillator strength of **e** is nearly 0. The observed bands may thus be attributed to the HOMO → LUMO (E_1^{exc} = 1.88 eV, f_1 = 0.0219) and the HOMO-1 → LUMO (E_2^{exc} = 3.32 eV, f_2 = 0.0065) transitions of **d**.

Geometry **a** of Ph_3N−TCNE was favored over **b** and best fit the spectrum. The same is true of Ph_3N−CA, which exhibits a maximum near 1.94 eV that can be associated with the HOMO → LUMO transition (E^{exc} = 1.96 eV, f = 0.0436). Structure **b** is considerably less stable, with a much longer D−A separation, and is unlikely to exist in the solution, particularly because there does not appear to be a second band in the spectrum of Ph_3N−CA.

Unlike PTh−TCNE where structure **d** was clearly preferred energetically, conformers **c** and **d** examined for PTh−CA are fairly close in energy. The PTh−CA complex has a high intensity absorption maximum near 1.60 eV. Only for structure **d** are the computed spectral data (E^{exc} = 1.46 eV, f = 0.0212) consistent with this experimental observation. Small values of *f* are characteristic of all transitions except for the HOMO → LUMO of **d**, for which the excitation energy matches the observed transition. Concerning MADO−CA, the calculations yield a binding energy of 0.01 kcal/mol and an intermolecular separation of 3.86 Å. This very weak binding may explain the fact that no CT band is observed in the spectrum of MADO−CA.

As a final and more general note, compared to the absorption bands of D−TCNE, those of D−CA are blue-shifted, consistent with the higher-lying LUMO in CA as compared to that in TCNE. CA is also bound more weakly to these electron donors than is TCNE, along with longer intermolecular separations.

4. Conclusions

For complexes of $PhNH_2$, *p*-$BrPhNH_2$, and DMBrA with TCNE, the lowest-energy conformation has the acceptor's double bond parallel with the 1,4-carbon atom line in the benzene ring. The appearance of a second CT band (which remains uncertain) would indicate the simultaneous presence of a second conformation, wherein one molecule is rotated 90° relative to the other. The addition of the Br atom weakens the $PhNH_2$−A interaction, which is, however, increased by the two methyl groups of DMBrA. The change of acceptor from TCNE to chloranil weakens the interactions uniformly. Moreover, the energy difference between the two conformations is lowered, which explains the clear presence of both isomers in the observed spectra.

The most probable geometry for carbazole complexes has the acceptor molecule above one of the phenyl rings. For acceptor TCNE, the double bond again lies parallel to the 1,4-carbon atom line in the ring, although this is not so clear cut for chloranil. This result is consistent with the observed spectra. The broad visible CT band is attributed to overlapping CT transitions arising from the HOMO and HOMO-1 of CBZ. The opening of the central ring in Ph_2NH leads to complexes exhibiting two well-separated absorption bands that correspond to the HOMO → LUMO and HOMO-1 → LUMO transitions. As in the case of carbazole, the acceptor molecule lies above one of the phenyl rings of Ph_2NH.

The absorption spectrum of Ph_3N−A contains only one CT band, which is attributed to the HOMO → LUMO transition, in a conformation wherein the A lies above one of the three phenyl rings. The other symmetric, rotated model is energetically unfavorable in Ph_3N−CA. The acceptor molecule lies above one of the phenyl rings of the donor in both PTh−A and MADO−A. The binding of MADO with CA is very weak, perhaps leading to the absence of a CT spectrum for this complex.

It should be pointed that although the calculated most probable geometries are responsible for the absorption maxima

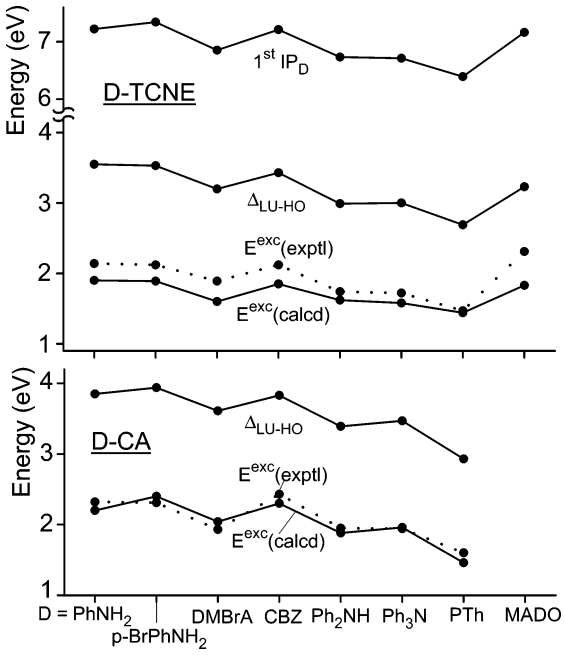

Figure 8. Schematic illustration of calculated and experimental excitation energies E^{exc} (lowest) for the D−TCNE and D−CA complexes. The LUMO−HOMO energy gaps, Δ_{LU-HO}, and the donor's first ionization potentials, 1st IP_D, are also shown for comparison.

other geometric conformations of the complex may not be ruled out in view of the "soft" or weak nature of the intermolecular bond. For some complexes, various orientational isomers may coexist in solution because of the ease of rotational interconversion among them;[23,26] they may contribute to the broadness and intensity of the CT adsorption.[23] The present DFT calculations provide a theoretical explanation of the energetics and origins of the CT spectra.

According to Mulliken,[2] a linear correlation is to be expected between the ionization potentials (IP) of donors and the excitation energies (E^{exc}) of the corresponding complexes with a given acceptor. Figure 8 illustrates the calculated and experimental excitation energies E^{exc} (lowest) for the D−TCNE and D−CA complexes, along with the first IPs calculated for the donors (1st IP_D). This Figure shows that E^{exc} parallels not only the 1st IP_D but also the LUMO−HOMO energy gap, Δ_{LU-HO}.

Acknowledgment. This work was supported by grant DAAD19-99-1-0206 to S.S. from the Army Research Office.

References and Notes

(1) Haga, N.; Nakajima, H.; Takayanagi, H.; Tokumaru, K. *J. Org. Chem.* **1998**, *63*, 5372.
(2) Mulliken, R. S.; Person, W. B. *Molecular Complexes: A Lecture and Reprint Volume*; Wiley & Sons: New York, 1969.
(3) Kroll, M. *J. Am. Chem. Soc.* **1968**, *90*, 1097.
(4) Dewar, M. J. S.; Lepley, A. R. *J. Am. Chem. Soc.* **1961**, *83*, 4560.
(5) Lippert, J. L.; Hanna, M. W.; Trotter, P. J. *J. Am. Chem. Soc.* **1969**, *91*, 4035.
(6) Morokuma, K. *Acc. Chem. Res.* **1977**, *10*, 294.
(7) Røeggen, I.; Dahe, T. *J. Am. Chem. Soc.* **1992**, *114*, 511.
(8) Matsuo, T.; Higuchi, O. *Bull. Chem. Soc. Jpn.* **1968**, *41*, 518.
(9) Chałsiński, G.; Szcześniak, M. M. *Chem. Rev.* **1994**, *94*, 1723.
(10) Scheiner, S. *Annu. Rev. Phys. Chem.* **1994**, *45*, 23.
(11) Kar, T.; Scheiner, S.; Cuma, M. *J. Chem. Phys.* **1999**, *111*, 849.
(12) Vosko, S. H.; Wilk, L.; Nusair, M. *Can. J. Phys.* **1980**, *58*, 1200.
(13) Lee, C.; Yang, W.; Parr, R. G. *Phys. Rev. B* **1988**, *37*, 785.
(14) Perdew, J. P.; Chevary, J. A.; Vosko, S. H.; Jackson, K. A.; Pederson, M. R.; Singh, D. J.; Fiolhais, C. *Phys. Rev. B* **1992**, *46*, 6671.
(15) Becke, A. D. *J. Chem. Phys.* **1993**, *98*, 1372.
(16) Becke, A. D. *J. Chem. Phys.* **1993**, *98*, 5648.
(17) Lacks, D. J.; Gordon, R. G. *Phys. Rev. A* **1993**, *47*, 4681.
(18) Adamo, C.; Barone, V. *J. Comput. Chem.* **1998**, *19*, 418.
(19) Adamo, C.; Barone, V. *J. Chem. Phys.* **1998**, *108*, 664.
(20) Ruiz, E.; Salahub, D. R.; Vela, A. *J. Phys. Chem.* **1996**, *100*, 12265.
(21) Frey, J. E.; Andrews, A. M.; Ankoviac, D. G.; Beaman, D. N.; Du Pont, L. E.; Elsner, T. E.; Lang, S. R.; Zwart, M. A. O.; Seagle, R. E.; Torreano, L. A. *J. Org. Chem.* **1990**, *55*, 606.
(22) (a) Foster, R. *Organic Charge-Transfer Complexes*; Academic Press: London, 1969; Chapter 8. (b) Rosokha, S. V.; Kochi, J. K. *J. Org. Chem.* **2002**, *67*, 1727.
(23) Edwards, W. D.; Du, M.; Royal, J. S.; McHale, J. L. *J. Phys. Chem.* **1990**, *94*, 5748.
(24) Frey, J. E.; Cole, R. D.; Kitchen, E. C.; Suprenant, L. M.; Sylwestrzak, M. S. *J. Am. Chem. Soc.* **1985**, *107*, 748.
(25) Landman, U.; Ledwith, A.; Marsh, D. G.; Williams, D. J. *Macromolecules* **1976**, *9*, 833.
(26) Kuroda, H.; Amano, T.; Ikemoto, I.; Akamatu, H. *J. Am. Chem. Soc.* **1967**, *89*, 6056.
(27) Frisch, M. J.; Trucks, G. W.; Schlegel, H. B.; Scuseria, G. E.; Robb, M. A.; Cheeseman, J. R.; Zakrzewski, V. G.; Montgomery, J. A., Jr.; Stratmann, R. E.; Burant, J. C.; Dapprich, S.; Millam, J. M.; Daniels, A. D.; Kudin, K. N.; Strain, M. C.; Farkas, O.; Tomasi, J.; Barone, V.; Cossi, M.; Cammi, R.; Mennucci, B.; Pomelli, C.; Adamo, C.; Clifford, S.; Ochterski, J.; Petersson, G. A.; Ayala, P. Y.; Cui, Q.; Morokuma, K.; Malick, D. K.; Rabuck, A. D.; Raghavachari, K.; Foresman, J. B.; Cioslowski, J.; Ortiz, J. V.; Stefanov, B. B.; Liu, G.; Liashenko, A.; Piskorz, P.; Komaromi, I.; Gomperts, R.; Martin, R. L.; Fox, D. J.; Keith, T.; Al-Laham, M. A.; Peng, C. Y.; Nanayakkara, A.; Gonzalez, C.; Challacombe, M.; Gill, P. M. W.; Johnson, B. G.; Chen, W.; Wong, M. W.; Andres, J. L.; Head-Gordon, M.; Replogle, E. S.; Pople, J. A. *Gaussian 98*; Gaussian, Inc.: Pittsburgh, PA, 1998.
(28) (a) Miertus, S.; Scrocco, E.; Tomasi, J. *Chem. Phys.* **1981**, *55*, 117. (b) Miertus, S.; Tomasi, J. *Chem. Phys.* **1982**, *65*, 239. (c) Cossi, M.; Barone, V.; Cammi, R.; Tomasi, J. *Chem. Phys. Lett.* **1996**, *255*, 327.
(29) Liao, M.-S.; Lu, Y.; Scheiner, S. *J. Comput. Chem.* **2003**, *24*, 623.
(30) Rosa, A.; Ricciardi, G.; Baerends, E. J.; van Gisbergen, S. J. A. *J. Phys. Chem. A* **2001**, *105*, 3311.
(31) (a) Nguyen, K. A.; Pachter, R. *J. Chem. Phys.* **2001**, *114*, 10757. (b) Nguyen, K. A.; Pachter, R. *J. Chem. Phys.* **2003**, *118*, 5802.
(32) Adamo, C.; Barone, V. *Theor. Chem. Acc.* **2000**, *105*, 169.
(33) Rathore, R.; Lindeman, S. V.; Kochi, J. K. *J. Am. Chem. Soc.* **1997**, *119*, 9393.
(34) Maverick, E.; Trueblood, K. N.; Bekoe, D. A. *Acta Crystallogr., Sect. B* **1978**, *34*, 2777.
(35) (a) Harding, T. T.; Wallwork, S. C. *Acta Crystallogr.* **1955**, *8*, 878. (b) Jones, N. D.; Marsh, R. E. *Acta Crystallogr.* **1962**, *15*, 809.
(36) Uno, B.; Okumura, N.; Seto, K. *J. Phys. Chem. A* **2000**, *104*, 3064.
(37) Wise, K. E.; Wheeler, R. A. *J. Phys. Chem. A* **1999**, *103*, 8279.
(38) Egolf, D. S.; Waterland, M. R.; Kelley, A. M. *J. Phys. Chem. B* **2000**, *104*, 10727.
(39) Okamoto, K.-i.; Ozeki, M.; Itaya, A.; Kusabayashi, S.; Mikawa, H. *Bull. Chem. Soc. Jpn.* **1975**, *48*, 1362.
(40) Klöpffer, W. *Z. Naturforsch., A* **1969**, *24*, 1923.
(41) Foster, R.; Hanson, P. *Biochim. Biophys. Acta* **1966**, *112*, 482.